Available online at www.sciencedirect.com
ScienceDirect
Journal of Sound and Vibration 314 (2008) 821–836
JOURNAL OF SOUND AND VIBRATION
www.elsevier.com/locate/jsvi

A space-averaged quadratic method for predicting one-dimensional power transfers

Cédric Devaux*, Nicolas Joly, Jean-Claude Pascal

Laboratoire d'Acoustique de l'Université du Maine, CNRS, Avenue Olivier Messiaen, 72085 Le Mans Cedex 9, France

Received 11 December 2006; received in revised form 25 December 2007; accepted 2 January 2008
Handling Editor: L.G. Tham
Available online 7 March 2008

Abstract

A method, which is based on space-averaged quadratic variables and does not assume the restrictive assumptions of the Statistical Energy Analysis (SEA) such as high overlap or damping conditions, is described. The results are spatially more detailed than an SEA response, and of a lower computational cost than the one of the usual displacement formulation. Some of the quadratic variables used, like energy densities or structural intensity, retain a strong energy meaning, even when time- and space-averaged. Their governing equation is derived for a homogeneous and isotropic medium with hysteretic damping. The main originality of this work lies in considering complex structural intensity and establishing appropriate energetic boundary conditions for both active and reactive space-averaged structural intensities by using the usual boundary conditions for the displacement field and the stress tensor. The numerical examples prove that this space-averaged quadratic method is well suited to describe global energy transfers along one-dimensional dissipative structures in a frequency range for which the overlap is too low to obtain a quadratic response from the SEA and solving the wave equation by using the Finite Element Method (FEM) would require more elements. Besides, describing junctions with impedances makes the resonant behaviour of the system still accessible on frequency responses.

1. Introduction

Vibration and noise predictive tools are necessary to define noise paths and implement efficient control strategies, for example in the automotive and aerospace industries. Unfortunately, it is difficult to predict the vibration behaviour of structures consisting of numerous connected elements correctly throughout the entire audible frequency range by a single predictive tool.

In a low-frequency range, the wave equation is usually solved by the Finite Element Method (FEM) and the Boundary Element Method (BEM). But the wavelength of the system deformation becomes shorter as the frequency increases and solving the wave equation by FEM or BEM would require the use of an excessive number of degrees of freedom. Furthermore, the sensitivity of the system to manufacturing imperfections

*Corresponding author.
E-mail address: cedric.devaux@univ-lemans.fr (C. Devaux).

0022-460X/$ - see front matter © 2008 Elsevier Ltd. All rights reserved.
doi:10.1016/j.jsv.2008.01.016

means that the FEM results for an ''ideal'' system may be very different from the behaviour of the manufactured product [1–3].

The analysis of mid- to high-frequency vibrations of structures has been an area of intense research for the past decades. Statistical Energy Analysis (SEA) [4] can provide an averaged space and frequency determination of a quadratic vibro-acoustical response ''in the statistical sense'' for the dynamic problem at high frequencies for complex built-up systems, assuming that the subsystems are weakly coupled [5]. But SEA is surely not appropriate to study the longitudinal waves in a broad frequency range in a wave guide, at least if one does not assume that the damping is so high to permit the system to have a high overlap.

This study deals with the application of energy methods for modelling structural dynamics and known as the vibrational conductivity analogy. This work is an extension of those energy methods as it accounts for both active and reactive parts of energy fields.

The oldest technique is the application of geometrical optics in engineering mechanics [6], and for which the energy density of a highly oscillating wave field is the solution of a transport equation. In the limit of a small transport mean free path, transport equations can be approached by diffusion equations. This is the approximation used by Rybak [7,8] for elastic waves which constitutes the basis of the vibrational conductivity analogy. A diffusion equation of the heat conduction type for the total energy density of a vibrating system can also be derived assuming that the high-frequency acoustic energy flow or the structural intensity is proportional to the gradient of energy density [9]. Further investigations of the energy model of rods and beams [10,11], membranes [12] and plates [13–15] were conducted.

Although this model was applied with success to one-dimensional structures [16], its justification is more difficult and its validity is not satisfying for multidimensional problems. In a semi-infinite case, the solutions are inconsistent with the exact power flow results [17]. Moreover, the thermal analogy is not correct for two-dimensional systems [18]; in particular, for a load point the far field solution of the diffusion equation is proportional to $1/\sqrt{r}$ while the exact solution is proportional to $1/r$. This statement shows that the thermal analogy can be applicable only to reverberant systems in which many reflections enable the interferences between various waves to be neglected.

The purpose of this paper is to present a method for describing power transfers along a one-dimensional dissipative structure in a frequency range for which solving the wave equation by using FEM would require a higher level of discretization and SEA cannot apply because of too many restrictive assumptions (high overlap, damping conditions). The approach consists in deriving averaged energy quantities to simplify their spatial description by removing useless details. The method uses a differential equation for the complex amplitude of the structural intensity, which remains valid in the case of high dissipative medium. In case of slight damping, some simplifications lead to results which are similar to the high-frequency equation of the vibrational conductivity analogy. One of the originalities of this work lies in considering complex structural intensity, which is generally not the case in the literature. This approach makes it possible to account for the usually ignored reactive effects, in particular by the methods which neglect the wave interferences. Besides, the method relies on exact energetic boundary conditions involving useful structural dynamics parameters like impedances and input powers, which contain displacement information and provide access to the resonances of the system.

The paper is organized as follows: the next section describes concepts like quadratic superposition and length scales of energy variables, showing how appropriate it is to use space averages to describe power transfers at a large length scale. In the same section, the link between large-scale components of energy variables and their space-averaged values is established for any damping value. Then exact and general boundary conditions for both active and reactive space-averaged structural intensities are obtained from the displacement formulation in Section 3, either for passive or active junctions. Finally, numerical examples are given in Section 4.

2. Space-averaged quadratic variables

2.1. General form of the displacement field and energy quantities

The systems considered in this work are one-dimensional systems in which only longitudinal waves propagate. Such systems can be qualified by only a complex elastic parameter $\lambda + 2\mu$, but the method

presented here is also applicable to other types of plane waves like quasi-longitudinal ones or shear horizontal ones in semi-infinite plates, or to acoustics by using the speed of sound c to link the wavenumber k to the angular frequency ω: $k = \omega/c$. Only general and non-restrictive assumptions are put forward:

- small displacement and small strain,
- homogeneous and isotropic medium with hysteretic damping (density ρ, damping factor η, complex Lamé coefficients $\lambda = \lambda_0(1 + j\eta)$ and $\mu = \mu_0(1 + j\eta)$),
- steady-state harmonic waves of angular frequency $\omega = 2\pi f$,
- system with large dimensions compared to the wavelength λ_0.

The displacement vector $\mathbf{u}$ derives from the scalar potential ϕ. Outside exciting sources the scalar potential ϕ and the displacement $\mathbf{u} = \mathbf{grad}\,\phi$ satisfy the scalar and the vectorial Helmholtz equation, respectively, $(\Delta + k^2)\phi = 0$ and $(\Delta + k^2)\mathbf{u} = 0$, where the wavenumber is $k = \sqrt{\rho\omega^2/(\lambda + 2\mu)}$. Hence, the complex amplitude u of the displacement field between two junctions is written as

$$u(x) = Ae^{-jkx} + Be^{jkx}, \tag{1}$$

where A and B are the complex amplitudes, respectively, of the forwards and the backward-propagating wave. Writing the wavenumber $k = k_0(1 - j\theta)$ leads to $k_0 = \sqrt{\rho\omega^2\eta^2/(2(\lambda_0 + 2\mu_0)(1 + \eta^2)(\sqrt{1 + \eta^2} - 1))}$ and $\theta = (\sqrt{1 + \eta^2} - 1)/\eta$. Among the quadratic variables are the kinetic energy density T, the strain energy density U, the total energy density $W = T + U$, the Lagrangian energy density $L = T - U$ and the structural intensity $\mathbf{I}$. Considering time-averaged quadratic variables and omitting the real part symbol, the amplitudes of T, U, W, L and $\mathbf{I}$ are obtained from the displacement field, which is detailed in Table 1, where $*$ denotes the conjugate number and $_{,x}$ the spatial derivative.

For example the complex strain energy density U can be written as

$$U(x) = \frac{\lambda + 2\mu}{4} kk^* \begin{pmatrix} AA^* e^{-j(k-k^*)x} + BB^* e^{j(k-k^*)x} \\ +A^* B e^{-j(k+k^*)x} + AB^* e^{j(k+k^*)x} \end{pmatrix}. \tag{2}$$

Its real part $\mathrm{Re}(U)$ is the "stocked" energy density whereas its imaginary part $\mathrm{Im}(U)$ is proportional to the "dissipated" power. The kinetic energy density T is an exception as it is the only purely real quadratic quantity among those presented in Table 1. Time averages of quadratic variables are governed by two wavenumbers: $k + k^*$ and $k - k^*$. These two wavenumbers match with two different scales of variation (Fig. 1): (i) the real wavenumber $k + k^*$ arises from interferences between propagative waves and characterizes stationary components of quadratic variables at the scale of the half-wavelength $\lambda_0/2 = 2\pi/(k + k^*)$ and (ii) the imaginary wavenumber $k - k^*$ characterizes the evanescence, due to the dissipation, of the large-scale components of quadratic variables, that is to say quadratic components built from plane waves when taken separately, like the first two terms of the expanded form (2) with amplitudes AA^* and BB^*. Hence, $k - k^*$ is the wavenumber that describes power transfers on a large scale compared to the wavelength.

Identifying the extreme values of energy densities, which are due to the positions of nodes and antinodes, is not useful in the frequency range this paper focuses on. Only components that describe power transfers on a large scale compared to the wavelength by giving the average level of energy quantities must be retained.

Table 1
Complex amplitudes of energy variables

Structural intensity	$I = j\omega(\lambda + 2\mu)u_{,x}u^*/2$
Kinetic energy density	$T = \rho\omega^2 uu^*/4$
Strain energy density	$U = (\lambda + 2\mu)u_{,x}u^*_{,x}/4$
Total energy density	$W = T + U$
Lagrangian density	$L = T - U$

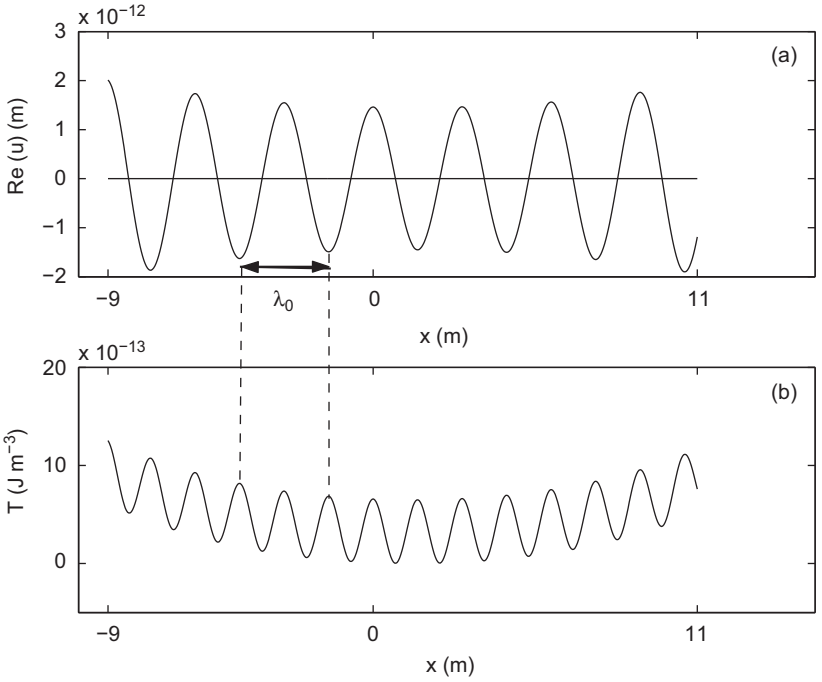

Fig. 1. One-dimensional longitudinal counter-propagative waves out from exciting sources in a steel medium (medium 1 in Table 6 except damping factor $\eta = 0.08$) at 2000 Hz: (a) real part of the displacement u; (b) kinetic energy density T.

2.2. Space-averaged variables and large-scale components for one-dimensional plane waves

At the scale of the half-wavelength $\lambda_0/2 = 2\pi/(k + k^*)$, the space average of any quadratic variable $\langle Q \rangle$ is defined as follows:

$$\langle Q \rangle(x) = \frac{2}{\lambda_0} \int_{x-\lambda_0/4}^{x+\lambda_0/4} Q(u)\,\mathrm{d}u, \tag{3}$$

where $\lambda_0/2$ is also the scale of variation of small-scale components of Q (Fig. 1).

Large-scale components of quadratic variables, with wavenumber $k - k^*$ appearing in Eq. (2), are linked to their half-wavelength-scale space-averaged values defined by Eq. (3). This link is general but can be illustrated for the complex strain energy density U considering a case without any load where the complex amplitude u of the displacement field is given by Eq. (1) and U by Eq. (2). Using the definition (3) of the average, the space-averaged strain energy density $\langle U \rangle$ can be written as

$$\langle U \rangle(x) = \frac{\lambda + 2\mu}{4} kk^* (AA^* \mathrm{e}^{-\mathrm{j}(k-k^*)x} + BB^* \mathrm{e}^{\mathrm{j}(k-k^*)x}) f(\theta). \tag{4}$$

The factor $(\lambda + 2\mu)kk^*(AA^*\mathrm{e}^{-\mathrm{j}(k-k^*)x} + BB^*\mathrm{e}^{\mathrm{j}(k-k^*)x})/4$ stands for the strain energy density obtained when interferences between the two waves considered are neglected. For plane waves, neglecting interferences terms is equivalent to retaining nothing but the large-scale components of quadratic variables. Here this is obtained applying an averaging process.

The averaging process introduces the last factor of Eq. (4):

$$f(\theta) = \frac{\sinh(\pi\theta)}{\pi\theta}. \tag{5}$$

This factor depends on only the dissipative properties of the medium, and takes the form $f(\theta) = 1 + O(\eta^2)$ for slight damping.

The same process can be used to average the kinetic energy density: the space-averaged value $\langle T\rangle$ is proportional, with the factor $f(\theta)$, to the large-scale components of T:

$$\langle T\rangle(x) = \frac{\rho\omega^2}{4}(AA^*\mathrm{e}^{-\mathrm{j}(k-k^*)x} + BB^*\mathrm{e}^{\mathrm{j}(k-k^*)x})f(\theta). \tag{6}$$

Using $k^2 = \rho\omega^2/(\lambda+2\mu)$, the space-averaged strain energy density $\langle U\rangle$ is found to be proportional to the space-averaged kinetic energy density $\langle T\rangle$:

$$\langle U\rangle = \frac{1+\mathrm{j}\theta}{1-\mathrm{j}\theta}\langle T\rangle. \tag{7}$$

Therefore, the result is similar for the space-averaged total energy density $\langle W\rangle = \langle T\rangle + \langle U\rangle$, the space-averaged Lagrangian density $\langle L\rangle = \langle T\rangle - \langle U\rangle$ and also for the space-averaged structural intensity whose complex amplitude $\langle I\rangle$ can be written as

$$\langle I\rangle(x) = \frac{\lambda+2\mu}{2}\omega k(AA^*\mathrm{e}^{-\mathrm{j}(k-k^*)x} - BB^*\mathrm{e}^{\mathrm{j}(k-k^*)x})f(\theta). \tag{8}$$

2.3. Differential equation for the space-averaged structural intensity

Only the propagation of large-scale components of quadratic variables is considered here. It is clear from Eq. (8) that the complex space-averaged structural intensity $\langle I\rangle$ satisfies the following differential equation between junctions:

$$\Delta\langle I\rangle + (k-k^*)^2\langle I\rangle = 0. \tag{9}$$

Space-averaged energy densities $\langle T\rangle$, $\langle U\rangle$, $\langle W\rangle$ and $\langle L\rangle$ also satisfy this differential equation. Since the wavenumber $k-k^*$ is purely imaginary, the space-averaged structural intensity $\langle I\rangle$ is the evanescent solution of a propagation equation. Moreover, Eq. (9) can be written again as

$$\Delta\langle I\rangle - 4(\mathrm{Im}(k))^2\langle I\rangle = 0, \tag{10}$$

which is the same as the equation controlling the space-averaged far field displacement autospectrum for bending waves in Ref. [19] where the space average interval is a multiple of quarters of wavelengths. In the case of a slight damping, Eq. (9) can be written as

$$\Delta\langle I\rangle - \frac{\eta^2\omega^2}{c_g^2}\langle I\rangle = 0, \tag{11}$$

where the wave celerity c_g defined as $c_g^2 = \omega^2/k^2$ is in the form $c_g^2 = (\lambda_0+2\mu_0)/\rho$ when $\eta \ll 1$. This form (11) is the basic equation (here outside exciting sources) previously derived in many works, but only for the real part of the structural intensity, as explained in Section 1. As it has been shown in Ref. [20] that this equation can be derived from energy equations first presented in Ref. [21] if interferences between plane waves are neglected and/or appropriate space averages are performed, the method used to obtain Eq. (9) is not new. However, since no slight damping assumption has been put forward, Eq. (9) is available for any value of the damping loss factor η.

2.4. Space-averaged energy densities

Here the choice has been made to work with the space-averaged structural intensity $\langle I\rangle$ and other space-averaged quadratic variables $\langle T\rangle$, $\langle U\rangle$, $\langle W\rangle$ and $\langle L\rangle$ can be set off against $\langle I\rangle$. Similar to acoustics [22], the structural intensity and energy densities (Table 1) are linked by

$$I_{,x} = -2\mathrm{j}\omega(T-U) + P, \tag{12}$$

where the input power density P is linked to the external load amplitude f_x by

$$P = -\frac{\mathrm{j}\omega}{2}f_x u^*. \tag{13}$$

Averaging Eq. (12) and using the ratio between the space-averaged kinetic energy density $\langle T\rangle$ and the space-averaged strain energy density $\langle U\rangle$ from Eq. (7) leads to either $\langle T\rangle$ or $\langle U\rangle$. Since the next section of this work will start dealing with a concentrated load at $x=a$, in such a case $\langle T\rangle$ can be written as

$$\langle T\rangle = -\left(\frac{1-\mathrm{j}\theta}{4\omega\theta}\right)(\langle I\rangle_{,x} - P\delta_a), \tag{14}$$

where δ_a is the Dirac function at $x=a$. Outside exciting sources, the space-averaged kinetic energy density $\langle T\rangle$ is proportional to the spatial derivative $\langle I\rangle_{,x}$ of the space-averaged structural intensity. Other averaged energy densities $\langle U\rangle$ (7), $\langle W\rangle$ and $\langle L\rangle$ are derived from $\langle T\rangle$.

3. Boundary conditions

Space-averaged quadratic quantities, first $\langle I\rangle$ and then $\langle T\rangle$, $\langle U\rangle$, $\langle W\rangle$ and $\langle L\rangle$, are obtained by solving the local equation (9) with appropriate boundary conditions for either passive or active junctions and which are presented in this section.

3.1. Active junctions

Considering a concentrated load f_x at $x=a$, the displacement potential ϕ satisfies

$$(\Delta + k^2)\phi(x) = -\frac{k^2 f_x}{\rho\omega^2} H(x-a), \tag{15}$$

where $H(x)$ is the Heaviside function.

Hence, the displacement potential ϕ can be written as

$$\phi(x) = C_1\cos(kx) + C_2\sin(kx) + \frac{f_x}{\rho\omega^2} H(x-a)(\cos(k(x-a)) - 1). \tag{16}$$

At $x=a$ where the concentrated load is f_x, $\langle I\rangle$ and $\langle I\rangle_{,x}$ are discontinuous. The input power density P (13) is an appropriate parameter expected to appear in boundary conditions for active junctions. The two-mentioned conditions concern the left limit value $\langle I\rangle(a^-)$ and the right limit value $\langle I\rangle(a^+)$: the active junction will be qualified by $\langle I\rangle(a^+) - \langle I\rangle(a^-)$ and $\langle I\rangle(a^+)/\langle I\rangle(a^-)$. These two numbers are computed from the complex amplitude of the displacement u, whose potential ϕ satisfies the motion equation (15) and can be written in the form (16). The complex amplitude of the displacement u is given by the derivation of the potential ϕ. In the same manner the complex amplitude of the spatial derivative of the displacement is given by the derivation of u. The complex amplitude of the structural intensity I is obtained from the displacement field (see Table 1).

The expanded complex amplitude of I contains the two kinds of components (wavenumbers $\pm(k+k^*)$ and $\pm(k-k^*)$ presented in Section 2.1) of the structural intensity. Since the space-averaged structural intensity $\langle I\rangle$ is proportional to the large-scale components (wavenumbers $\pm(k-k^*)$) of the structural intensity, $\langle I\rangle$ can be extracted from I.

Terms which are factors of the Heaviside function $H(x-a)$ in the expression of $\langle I\rangle$ give the jump of the amplitude of the space-averaged structural intensity at $x=a$:

$$\langle I\rangle(a^+) - \langle I\rangle(a^-) = f(\theta)\frac{\mathrm{j}\omega}{4}\frac{(\lambda+2\mu)k^2}{\rho\omega^2}\begin{pmatrix}\dfrac{k^*}{k}f_x^*(-C_1 k\sin(ka) + C_2 k\cos(ka))\\ +f_x\left(C_1^* k^*\sin(k^*a) - C_2^* k^*\cos(k^*a)\right)\end{pmatrix}. \tag{17}$$

Expression (17) contains the complex amplitude of the displacement at $x=a$ and can be written again as

$$\langle I\rangle(a^+) - \langle I\rangle(a^-) = \frac{f(\theta)}{2}\left(-\frac{\mathrm{j}\omega}{2}f_x u^*(a) + \frac{k^*}{k}\frac{\mathrm{j}\omega}{2}f_x^* u(a)\right), \tag{18}$$

or, using definition (13) of the input power density P:

$$\langle I\rangle(a^+) - \langle I\rangle(a^-) = \frac{P}{2}\left(1 + \frac{k^*}{k}\frac{P^*}{P}\right)f(\theta), \tag{19}$$

which is the first boundary condition qualifying the active junction. This last expression (19) is more complicated than the single input power density P which gives the discontinuity of the local structural intensity: $I(a^+) - I(a^-) = P$. In particular it involves the loss factor θ which is present in $f(\theta)$ due to the space average and in $k^*/k = (1 + \mathrm{j}\theta)/(1 - \mathrm{j}\theta)$.

The second boundary condition deals with the ratio $\langle I\rangle(a^+)/\langle I\rangle(a^-)$. This ratio can be written as

$$\frac{\langle I\rangle(a^+)}{\langle I\rangle(a^-)} = 1 + \frac{\langle I\rangle(a^+) - \langle I\rangle(a^-)}{\langle I\rangle(a^-)}. \tag{20}$$

The left limit value of the space-averaged structural intensity $\langle I\rangle(a^-)$ can be computed from the expression of $\langle I\rangle$. With $(\lambda + 2\mu)/(\lambda^* + 2\mu^*) = k^{*2}/k^2$, it can be written as

$$\langle I\rangle(a^-) = \frac{f(\theta)}{2}\left(I(a^-) + \frac{k^*}{k}I^*(a^-)\right). \tag{21}$$

At $x = -L_1$ the impedance Z_1 is defined as $Z_1 = (\lambda + 2\mu)u_{,x}(-L_1)/(\mathrm{j}\omega u(-L_1))$ and is linked to the specific impedance z_1 by $Z_1 = \rho c\, z_1$. At $x_0 = a^-$ the impedance Z_{a^-} can be computed by using z_1, as presented in the appendix. On the left side of the load point a, the normal derivative ∂/∂_n is $\partial/\partial_n = -\partial/\partial_x$ and the impedance Z_{a^-} can be written as

$$Z_{a^-} = \rho c\frac{\mathrm{e}^{\mathrm{j}k(L_1+a)} - \mathrm{e}^{-\mathrm{j}k(L_1+a)} + z_1(\mathrm{e}^{\mathrm{j}k(L_1+a)} + \mathrm{e}^{-\mathrm{j}k(L_1+a)})}{z_1(\mathrm{e}^{\mathrm{j}k(L_1+a)} - \mathrm{e}^{-\mathrm{j}k(L_1+a)}) - \mathrm{e}^{\mathrm{j}k(L_1+a)} - \mathrm{e}^{-\mathrm{j}k(L_1+a)}}. \tag{22}$$

Hence, the left limit value of the structural intensity $I(a^-)$ can be written as

$$I(a^-) = \frac{\mathrm{j}\omega^2}{2}Z_{a^-}u(a)u^*(a), \tag{23}$$

which, accounting for the input power density P (13), can be written as follows:

$$I(a^-) = 2\mathrm{j}Z_{a^-}\frac{PP^*}{f_x f_x^*}. \tag{24}$$

Using Eqs. (20), (21) and (24), the second boundary condition at $x = a$ deals with the ratio $\langle I\rangle(a^+)/\langle I\rangle(a^-)$ and finally can be written as

$$\frac{\langle I\rangle(a^+)}{\langle I\rangle(a^-)} = 1 + \frac{P\left(1 + \frac{k^*P^*}{kP}\right)}{2\mathrm{j}\frac{PP^*}{f_x f_x^*}\left(Z_{a^-} - \frac{k^*Z_{a^-}^*}{k}\right)}. \tag{25}$$

3.2. Passive junctions

3.2.1. Impedance condition

The impedance condition of the complex amplitude of the displacement u is

$$u_{,n}(L) + \mathrm{j}kzu(L) = 0, \tag{26}$$

where $_{,n}$ is the normal derivative and z is the specific impedance at $x = L$: $z = z_1$ when $L = -L_1$ and $z = z_2$ when $L = L_2$. Between junctions, when $-L_1 \leqslant x < a$ or $a < x \leqslant L_2$, the complex amplitude u satisfies the Helmholtz equation and is written in the form (1).

Using Eq. (26) the link between the two constants A and B of the displacement (1) can be found:

$$A = \frac{\varepsilon + z}{\varepsilon - z}\mathrm{e}^{2\mathrm{j}kL}B, \tag{27}$$

where the parameter $\varepsilon = \pm 1$ is defined by

$$\frac{\partial}{\partial n} = \varepsilon \frac{\partial}{\partial x}. \tag{28}$$

Writing the amplitude of the space-averaged structural intensity $\langle I \rangle$ (9) and its spatial derivative $\langle I \rangle_{,x}$ at $x = L$ gives

$$\langle I \rangle_{,x}(L) - \mathrm{j}(k - k^*)\frac{1+\alpha}{1-\alpha}\langle I \rangle(L) = 0, \tag{29}$$

where

$$\alpha = \frac{(\varepsilon + z)(\varepsilon + z^*)}{(\varepsilon - z)(\varepsilon - z^*)}. \tag{30}$$

Using definition (28) of ε, Eq. (29) leads to the following mixed boundary condition for the complex amplitude of the space-averaged structural intensity:

$$\langle I \rangle_{,n}(L) + \mathrm{j}(k - k^*)\frac{1+zz^*}{z+z^*}\langle I \rangle(L) = 0. \tag{31}$$

Particular cases of mixed boundary conditions with real specific impedances are presented in Table 2.

3.2.2. Discontinuity of the material density

3.2.2.1. Configuration and definition of impedances. Boundary conditions for a discontinuity of the material density at $x = d$ (Fig. 2) are explained in this section. Impedances and specific impedances involved in the computation of these boundary conditions are presented in Tables 3–5.

Using equations in Tables 3 and 4 that link concentrated loads f_{x_1} and f_{x_2} to strain discontinuities at $x = a$ and b, the three specific impedances z_{a^-}, z_a and z_{a+} and the three specific impedances z_{b^-}, z_b and z_{b+} are, respectively linked by $z_{a^+} + z_{a^-} = z_a$ and $z_{b^+} + z_{b^-} = z_b$.

3.2.2.2. Boundary conditions for the displacement field. The displacement and the normal stress are continuous at the boundary $x = d$ between the two media:

$$\begin{cases} u(d^-) = u(d^+), \\ (\lambda_1 + 2\mu_1)u_{,x}(d^-) = (\lambda_2 + 2\mu_2)u_{,x}(d^+). \end{cases} \tag{32}$$

3.2.2.3. Specific impedances on each side of the boundary. Both specific impedances z_{d^-} and z_{d^+} can be computed from other specific impedances, respectively, z_{a^+} and z_{b^-}, by using formula (49) of the appendix:

$$z_{d^-} = \frac{(1 - z_{a^+})\mathrm{e}^{-\mathrm{j}k_1(d-a)} - (1 + z_{a^+})\mathrm{e}^{\mathrm{j}k_1(d-a)}}{(1 - z_{a^+})\mathrm{e}^{-\mathrm{j}k_1(d-a)} + (1 + z_{a^+})\mathrm{e}^{\mathrm{j}k_1(d-a)}} \tag{33}$$

and

$$z_{d^+} = -\frac{(-1 - z_{b^-})\mathrm{e}^{-\mathrm{j}k_2(d-b)} - (-1 + z_{b^-})\mathrm{e}^{\mathrm{j}k_2(d-b)}}{(-1 - z_{b^-})\mathrm{e}^{-\mathrm{j}k_2(d-b)} + (-1 + z_{b^-})\mathrm{e}^{\mathrm{j}k_2(d-b)}}. \tag{34}$$

Table 2
Particular cases of mixed boundary conditions with real specific impedances

	Free end	Clamped end	Anechoic end
Specific impedance	$z = 0$	$\lvert z \rvert \to +\infty$	$z = 1$
Displacement	$u_{,n}(L) = 0$	$u(L) = 0$	$u_{,n}(L) + \mathrm{j}ku(L) = 0$
Space-averaged structural intensity	$\langle I \rangle(L) = 0$	$\langle I \rangle(L) = 0$	$\langle I \rangle_{,n}(L) + \mathrm{j}(k - k^*)\langle I \rangle(L) = 0$

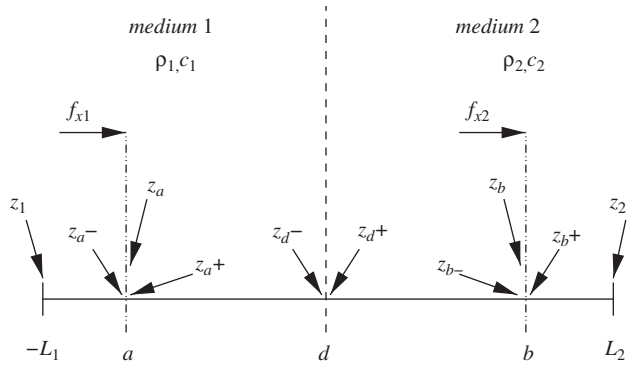

Fig. 2. Configuration of the studied system in Section 4.2.

Table 3
Definitions of impedances and specific impedances for the active junction at $x = a$

x	a^-	a	a^+
Impedance	$Z_{a^-} = -\dfrac{(\lambda_1 + 2\mu_1)u_{,x}(a^-)}{\mathrm{j}\omega u(a)}$	$Z_a = \dfrac{f_{x_1}}{\mathrm{j}\omega u(a)}$	$Z_{a^+} = \dfrac{(\lambda_1 + 2\mu_1)u_{,x}(a^+)}{\mathrm{j}\omega u(a)}$
Specific impedance	$z_{a^-} = \dfrac{Z_{a^-}}{\rho_1 c_1}$	$z_a = \dfrac{Z_a}{\rho_1 c_1}$	$z_{a^+} = \dfrac{Z_{a^+}}{\rho_1 c_1}$

Table 4
Definitions of impedances and specific impedances for the active junction at $x = b$

x	b^-	b	b^+
Impedance	$Z_{b^-} = \dfrac{(\lambda_2 + 2\mu_2)u_{,x}(b^-)}{\mathrm{j}\omega u(b)}$	$Z_b = \dfrac{f_{x_2}}{\mathrm{j}\omega u(b)}$	$Z_{b^+} = -\dfrac{(\lambda_2 + 2\mu_2)u_{,x}(b^+)}{\mathrm{j}\omega u(b)}$
Specific impedance	$z_{b^-} = \dfrac{Z_{b^-}}{\rho_2 c_2}$	$z_b = \dfrac{Z_b}{\rho_2 c_2}$	$z_{b^+} = \dfrac{Z_{b^+}}{\rho_2 c_2}$

Table 5
Definitions of impedances and specific impedances for the passive junction at $x = d$

x	d^-	d^+
Specific impedance	$z_{d^-} = \dfrac{u_{,x}(d^-)}{\mathrm{j}k_1 u(d^-)}$	$z_{d^+} = -\dfrac{u_{,x}(d^+)}{\mathrm{j}k_2 u(d^+)}$
Impedance	$Z_{d^-} = \rho_1 c_1 z_{d^-}$	$Z_{d^+} = \rho_2 c_2 z_{d^+}$

Moreover, both specific impedances z_{a^-} and z_{b^+} can be computed from other specific impedances, respectively, z_1 and z_2:

$$z_{a^-} = -\frac{(-1 - z_1)\mathrm{e}^{\mathrm{j}k_1(L_1+a)} - (-1 + z_1)\mathrm{e}^{-\mathrm{j}k_1(L_1+a)}}{(-1 - z_1)\mathrm{e}^{\mathrm{j}k_1(L_1+a)} + (-1 + z_1)\mathrm{e}^{-\mathrm{j}k_1(L_1+a)}}, \tag{35}$$

$$z_{b^+} = \frac{(1 - z_2)\mathrm{e}^{-\mathrm{j}k_2(L_2-b)} - (1 + z_2)\mathrm{e}^{\mathrm{j}k_2(L_2-b)}}{(1 - z_2)\mathrm{e}^{-\mathrm{j}k_2(L_2-b)} - (1 + z_2)\mathrm{e}^{\mathrm{j}k_2(L_2-b)}}. \tag{36}$$

As a consequence, knowing specific impedances z_{d^-} and z_{d^+} comes down to knowing specific impedances z_1 and z_2.

3.2.2.4. Boundary conditions for the space-averaged structural intensity. At $x = d$ the space-averaged structural intensity is continuous. Hence, the first boundary condition is

$$\langle I\rangle(d^+) = \langle I\rangle(d^-). \tag{37}$$

Since specific impedances z_{d^-} and z_{d^+} can be computed from specific impedances z_1 and z_2, mixed boundary conditions can be written for space-averaged structural intensities $\langle I\rangle(d^-)$ and $\langle I\rangle(d^+)$. These boundary conditions are the same kind as Eq. (31):

$$-\langle I\rangle_{,x}(d^-) + \mathrm{j}(k_1 - k_1^*)\frac{1 + z_{d^-} z_{d^-}^*}{z_{d^-} + z_{d^-}^*}\langle I\rangle(d^-) = 0, \tag{38}$$

$$\langle I\rangle_{,x}(d^+) + \mathrm{j}(k_2 - k_2^*)\frac{1 + z_{d^+} z_{d^+}^*}{z_{d^+} + z_{d^+}^*}\langle I\rangle(d^+) = 0. \tag{39}$$

The second boundary condition is related to the ratio $\langle I\rangle_{,x}(d^+)/\langle I\rangle_{,x}(d^-)$. This ratio can be obtained from Eqs. (37)–(39):

$$\frac{\langle I\rangle_{,x}(d^+)}{\langle I\rangle_{,x}(d^-)} = -\frac{k_2 - k_2^*}{k_1 - k_1^*}\frac{1 + z_{d^+} z_{d^+}^*}{1 + z_{d^-} z_{d^-}^*}\frac{z_{d^-} + z_{d^-}^*}{z_{d^+} + z_{d^+}^*}. \tag{40}$$

4. Application

The approach consists in solving Eq. (9) along the one-dimensional structure, with boundary conditions:

- Eqs. (19) and (25) for a concentrated load,
- Eq. (31) for a specific impedance z at the end of the system, and
- Eqs. (37) and (40) for a discontinuity of material density.

Once the space-averaged structural intensity $\langle I\rangle$ is obtained, space-averaged energy densities $\langle T\rangle$, $\langle U\rangle$, $\langle W\rangle$ and $\langle L\rangle$ are derived.

4.1. A first example dealing with active and passive junctions

Computations were carried out for pure longitudinal waves propagating between $-L_1 = -9\,\mathrm{m}$ and $L_2 = 11\,\mathrm{m}$ (Fig. 3) in a steel medium, where parameters are defined in Table 6 (medium 1). The concentrated load f_x is located at $a = 3\,\mathrm{m}$. The specific impedance $z_1 = 0.05 + 0.01\mathrm{j}$ indicates that the junction is highly reflecting and a little dissipative. The specific impedance $z_2 = 0.9$ indicates that the junction is slightly reflecting.

4.1.1. Frequency response for the space-averaged structural intensity

Power transfers can be analysed in the frequency domain. The active structural intensity is computed at $b = 7\,\mathrm{m}$ for a unitary load $f_x = 1\,\mathrm{Pa}$ (Fig. 4). The highest and lowest values are changing over.

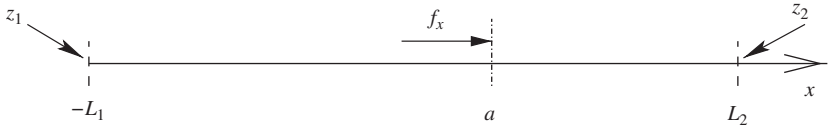

Fig. 3. Configuration of the studied system in Section 4.1.

Table 6
Properties of media

	Medium 1	Medium 2
Density, ρ (kg m^{-3})	7800	2700
Young's modulus, E (Pa)	$2.1\,10^{11}(1+\mathrm{j}0.01)$	$0.7\,10^{11}(1+\mathrm{j}0.01)$
Poisson ratio, v	0.3	0.3

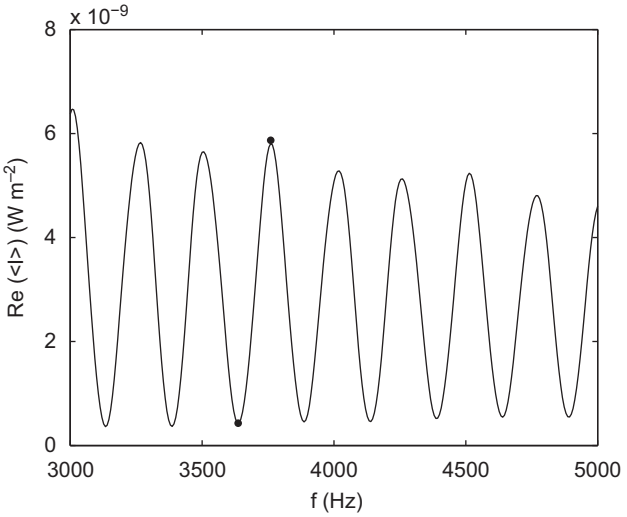

Fig. 4. Space-averaged active structural intensity at point $b = 7$ m (bold point of Figs. 5 and 6) for a unitary load f_x.

4.1.2. Spatial description of the power transfers

Exact energy quantities are computed from the displacement field whereas space-averaged energy quantities are computed using the averaged quadratic model presented in this work. The active structural intensity is computed at 3640 Hz (Fig. 5) for one of its lowest values and at 3750 Hz (Fig. 6) for one of its highest values (bold points of Fig. 4). These different levels are due to the extreme values of the input impedance modulus $|Z_a| = |Z_{a^+} + Z_{a^-}|$ defined in Table 3 (Fig. 7) and computed by using specific impedances z_1 and z_2. With the averaged quadratic formulation, the large-scale components of energy quantities are well reconstituted. When space-averaged, energy quantities like energy densities (14) and (7) become smoother (Fig. 6). A model based on the displacement with 6 finite element nodes per wavelength would require 76 nodes at 4000 Hz whereas very few nodes are necessary on $-L_1 \leqslant x \leqslant a$ and on $a \leqslant x \leqslant L_2$ for the space-averaged quadratic model presented in this work. This demonstrates the relevance of this averaged energy method as the frequency increases and many systems like this one (Fig. 3) are connected.

4.2. A second example dealing with a discontinuity of density

Computations were carried out for pure longitudinal waves propagating at a frequency of 4000 Hz either in a steel medium (Table 6) between $-L_1 = -10$ m and $d = 3$ m or in an aluminium medium (Table 6) between $d = 3$ m and $L_2 = 10$ m (Fig. 2). A first concentrated load $f_{x_1} = 1$ Pa is located at $a = -2$ m and a second one $f_{x_2} = 2$ Pa is located at $b = 7$ m. The specific impedance z_1 is $z_1 = 0.05 + 0.01\mathrm{j}$ as in Section 4.1. The specific impedance $z_2 = 0.1$ indicates that the junction at $x = L_2$ is highly reflecting. The discontinuity of the material density at $x = d$ implies a discontinuity of the spatial derivative of both local (computed from the displacement field) and space-averaged structural intensities. The averaged formulation enables a good reconstitution of the latter (Fig. 8).

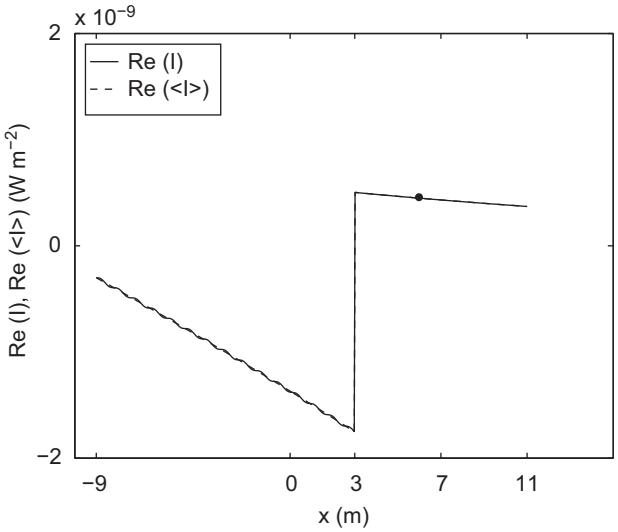

Fig. 5. Real part of the structural intensities at 3640 Hz.

5. Discussion

For energy variables of one-dimensional plane waves, the local structure of the energy field results in interferences between the counter-propagative waves. Performing space averages at the scale of the half-wavelength λ_0 leads to consideration of nothing but the transfer of large-scale components of quadratic variables. Although the assumption was not a priori made, this approach is similar to the decorrelation of the waves, which lends a statistical sense to the method, as performing frequency averages would do [19].

In the particular case of plane waves, this result can be extended to bi-dimensional and three-dimensional spaces: the interference field between two plane waves with a relative angle α, in the plane defined by both directions, a spatial pseudo-periodicity characterized by a cell of surface $S = \lambda_0^2/(4|\sin\alpha\cos\alpha|)$ [23]. Expressions (4), (6) and (8) for averaged energy variables can easily be extended for considering the combination of wave vectors instead of wavenumbers; relation (7) and the governing equation (9) then remain valid.

Real acoustic fields resulting from the superposition of exact propagative plane waves are, however, not common. Even for such an approximated acoustic field, the associated boundary conditions are not obvious, providing no clear sense to an extension of conditions (25), (31) or (40) for two- or three-dimensional spaces.

The averaging process used above is based on the pseudo-periodicity of the field. This property is no more satisfied by bending wave fields, because of the contribution of evanescent wave components. Hence, the direct extension of the presented approach to more complex one-dimensional waveguides, accounting for bending waves, seems to be difficult as evanescent components must be taken into account when establishing boundary conditions for energy variables.

6. Conclusion

Because of the wave vector combinations, quadratic variables in plane waves hold two different kinds of components. In a one-dimensional case, these two kinds of components match with two very different scale lengths: the smallest one is the size of the half-wavelength and results from interferences between propagative waves, whereas the largest one accounts for dissipative phenomena and global energy transfers on a large scale compared to the wavelength. The smaller the damping, the larger the size of global energy transfers.

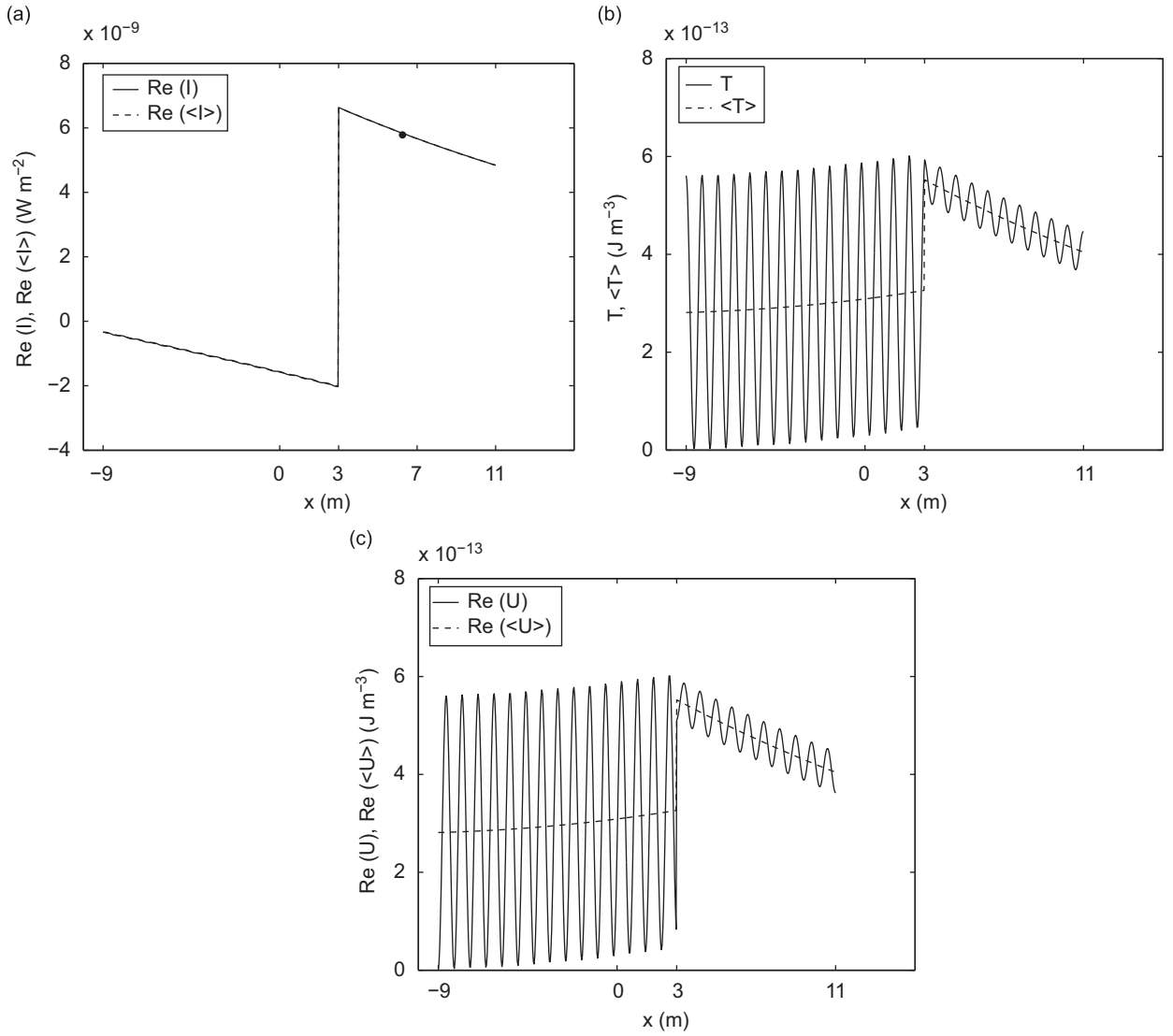

Fig. 6. Energy quantities at 3750 Hz: (a) real part of the structural intensities, (b) kinetic energy densities, (c) real part of the strain energy densities. Solid line: solution obtained from the displacement field; dashed line: solution obtained from the averaged quadratic method.

Performing space averages along a half-wavelength removes small-scale components of quadratic variables and enables the development of an energetic formulation as the frequency increases. Besides energetic boundary conditions for both active and reactive space-averaged structural intensities have been obtained from the displacement formulation for passive and active junctions described with impedances. Such characteristics make the present space-averaged quadratic formulation appropriate for modelling global energy transfers along one-dimensional dissipative structures in a middle frequency range. Performing space averages leads to a simplification of quadratic fields, so much so that this method requires less elements than solving the wave equation with FEM. Besides, the space average interval is well defined as the half-wavelength, which leads to a more space-detailed quadratic response than space averages on subsystems in SEA give, provided that the modal overlap is high enough for SEA to be used. Description of junctions with impedances is not only the clear difference between this work and previous ones but it also enables to access the frequency response of the input impedance.

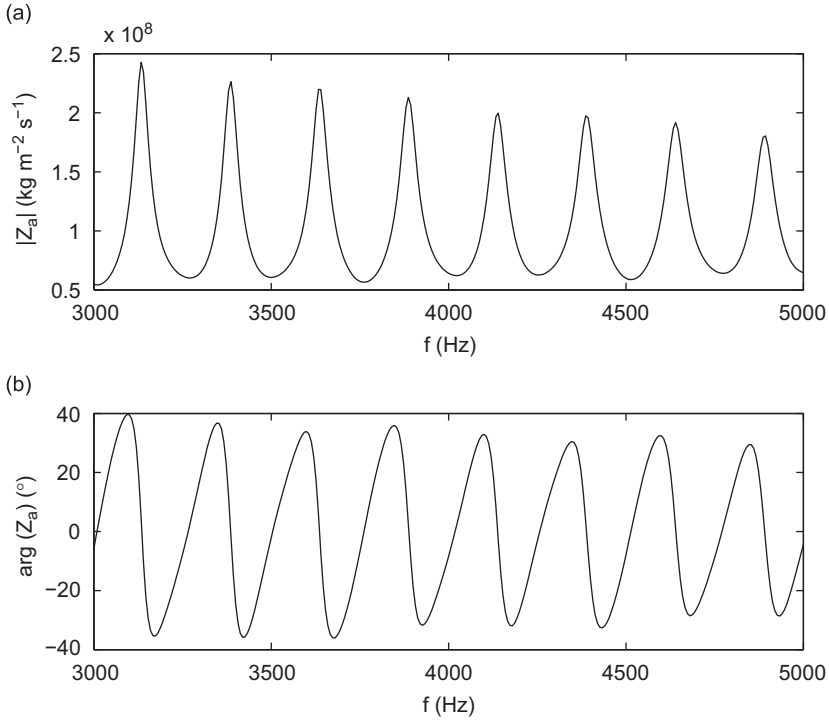

Fig. 7. Input impedance Z_a: (a) modulus $|Z_a|$; (b) angle $\arg(Z_a)$.

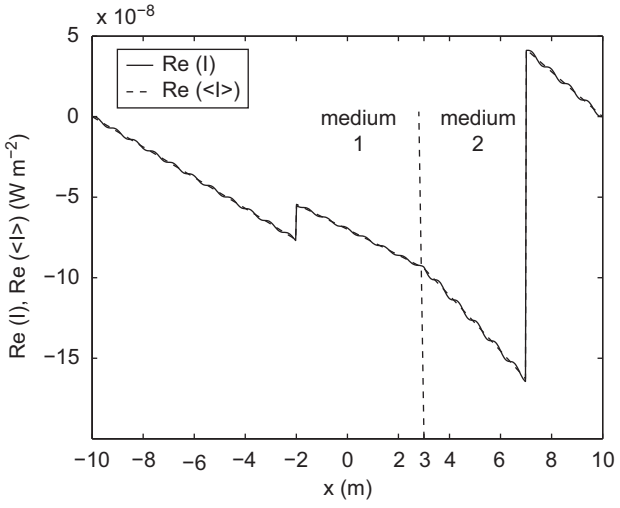

Fig. 8. Real part of the structural intensities. Solid line: solution obtained from the displacement field; dashed line: solution obtained from the averaged quadratic method.

Appendix A. Formula for computing impedances

Between $x = L$ and $x = x_0$, the displacement u is

$$u(x) = A_1 e^{jk(x-x_0)} + A_2 e^{-jk(x-x_0)}, \tag{41}$$

where A_1 and A_2 are constants. If z is the specific impedance at $x = L$, the mixed boundary condition for the displacement at $x = L$ is the impedance condition $u_{,n}(L) + \mathrm{j}kzu(L) = 0$ which is

$$\varepsilon(A_1 \mathrm{e}^{\mathrm{j}k(L-x_0)} - A_2 \mathrm{e}^{-\mathrm{j}k(L-x_0)}) = -z(A_1 \mathrm{e}^{\mathrm{j}k(L-x_0)} + A_2 \mathrm{e}^{-\mathrm{j}k(L-x_0)}), \tag{42}$$

where the parameter $\varepsilon = \pm 1$ is defined by

$$\frac{\partial}{\partial n} = \varepsilon \frac{\partial}{\partial x}. \tag{43}$$

From Eq. (41) the displacement u and its spatial derivative $u_{,x}$ at $x = x_0$ are

$$\begin{cases} u(x_0) = A_1 + A_2, \\ u_{,x}(x_0) = \mathrm{j}k(A_1 - A_2). \end{cases} \tag{44}$$

From Eq. (44) coefficients A_1 and A_2 can be written as functions of $u(x_0)$:

$$A_1 = \frac{(\varepsilon - z)u(x_0)\mathrm{e}^{-\mathrm{j}k(L-x_0)}}{\varepsilon(\mathrm{e}^{\mathrm{j}k(L-x_0)} + \mathrm{e}^{-\mathrm{j}k(L-x_0)}) + z(\mathrm{e}^{\mathrm{j}k(L-x_0)} - \mathrm{e}^{-\mathrm{j}k(L-x_0)})}, \tag{45}$$

$$A_2 = \frac{(\varepsilon + z)u(x_0)\mathrm{e}^{\mathrm{j}k(L-x_0)}}{\varepsilon(\mathrm{e}^{\mathrm{j}k(L-x_0)} + \mathrm{e}^{-\mathrm{j}k(L-x_0)}) + z(\mathrm{e}^{\mathrm{j}k(L-x_0)} - \mathrm{e}^{-\mathrm{j}k(L-x_0)})}. \tag{46}$$

Eqs. (45) and 46 give the impedance Z_{x_0} linking $u(x_0)$ and $u_{,x}(x_0)$ as

$$\mathrm{j}\omega Z_{x_0} u(x_0) = \varepsilon(\lambda + 2\mu)u_{,x}(x_0). \tag{47}$$

This impedance Z_{x_0} is

$$Z_{x_0} = \frac{\varepsilon(\lambda + 2\mu)k}{\omega} \frac{A_1 - A_2}{A_1 + A_2}, \tag{48}$$

which can be written as, introducing the wave celerity c:

$$Z_{x_0} = \varepsilon\rho c \frac{(\varepsilon - z)\mathrm{e}^{-\mathrm{j}k(L-x_0)} - (\varepsilon + z)\mathrm{e}^{\mathrm{j}k(L-x_0)}}{(\varepsilon - z)\mathrm{e}^{-\mathrm{j}k(L-x_0)} + (\varepsilon + z)\mathrm{e}^{\mathrm{j}k(L-x_0)}}. \tag{49}$$

References

[1] E. Rébillard, J.L. Guyader, Calculation of the radiated sound from coupled plates, *Acta Acustica* 86 (2000) 303–312.

[2] E. Capiez-Lernout, M. Pellissetti, H. Pradlwarter, G.I. Schueller, C. Soize, Data and model uncertainties in complex aerospace engineering systems, *Journal of Sound and Vibration* 295 (2006) 923–938.

[3] R.J. Bernhard, The limits of predictability due to manufacturing and environmentally induced uncertainty, *Proceedings of Internoise 96*, Liverpool, July 30–August 2 1996, pp. 2867–2872.

[4] R.H. Lyon, R.G. DeJong, *Theory and Application of Statistical Energy Analysis*, Butterworth-Heinemann, Boston, 1995.

[5] D.E. Newland, Calculation of power flow between coupled oscillators, *Journal of Sound and Vibration* 3 (1966) 262–276.

[6] C.R. Steele, Application of the WKB method in solid mechanics, in: S. Nemat-Nasser (Ed.), *Mechanics Today*, Pergamon Press, New York, 1976, pp. 243–295.

[7] S.A. Rybak, Waves in a plate containing random inhomogeneities, *Soviet Physics and Acoustics* 17 (1972) 345–349.

[8] S.A. Rybak, Randomly coupled flexural and longitudinal vibrations of plates, *Soviet Physics and Acoustics* 18 (1972) 76–79.

[9] D.J. Nefske, S.H. Sung, Power flow finite element analysis of dynamic systems: basic theory and applications to beams, *Journal of Vibration Acoustics Stress and Reliability in Design* 111 (1989) 94–100.

[10] J.C. Wohlever, R.J. Bernhard, Mechanical energy flow models of rods and beams, *Journal of Sound and Vibration* 153 (1) (1992) 1–19.

[11] Y. Lase, M.N. Ichchou, L. Jezequel, Energy flow analysis of bars and beams: theoretical formulations, *Journal of Sound and Vibration* 201 (5) (1996) 281–305.

[12] O. Bouthier, R.J. Bernhard, Simple models of energy flow in vibrating membranes, *Journal of Sound and Vibration* 182 (1995) 129–147.

[13] O. Bouthier, R.J. Bernhard, Simple models of energy flow in vibrating plates, *Journal of Sound and Vibration* 182 (1995) 149–164.

[14] R.J. Bernhard, O. Bouthier, Model of the space averaged energetics of plates, *AIAA Paper 90-3921*, 1990.

[15] M.N. Ichchou, L. Jezequel, Comments on simple models of the energy flow in vibrating membranes and transversaly vibrating plates, *Journal of Sound and Vibration* 195 (1996) 679–685.

[16] A. Bocquillet, M.N. Ichchou, L. Jezequel, Energetics of fluid-filled pipes up to high frequencies, *Journal of Fluid and Structures* 17 (2003) 491–510.
[17] J.T. Xing, W.G. Price, A power flow analysis based on continuum dynamics, *Proceedings of the London Royal Society A* 455 (1999) 401–436.
[18] R.S. Langley, On the vibrational conductivity approach to high frequency dynamics for two-dimensional structural components, *Journal of Sound and Vibration* 182 (4) (1995) 637–657.
[19] M. Djimadoum, J.L. Guyader, Vibratory prediction with an equation of diffusion, *Acta Acustica* 3 (1995) 11–24.
[20] A. Sestieri, A. Carcaterra, Space average and wave interference in vibration conductivity, *Journal of Sound and Vibration* 263 (2003) 475–491.
[21] A. Carcaterra, A. Sestieri, Energy density equations and power flow in structures, *Journal of Sound and Vibration* 188 (2) (1995) 269–282.
[22] P.W. Smith Jr., T.J. Schultz, C.I. Malme, Intensity measurement in near fields and reverberant spaces, *Bolt Beranek and Newman Inc. Report No. 1135*, 1964.
[23] N. Joly, J.-C. Pascal, Spatial averaging in energy methods: case of longitudinal plane waves, *Proceedings of the 11th International Congress of Sound and Vibration*, St. Petersburg, 5–8 July 2004, pp. 3645–3652.